

1-Aryl-3-(1-acylpiperidin-4-yl)urea Inhibitors of Human and Murine Soluble Epoxide Hydrolase: Structure–Activity Relationships, Pharmacokinetics, and Reduction of Inflammatory Pain

Tristan E. Rose, Christophe Morisseau, Jun-Yan Liu, Bora Inceoglu, Paul D. Jones, James R. Sanborn, and Bruce D. Hammock*

Department of Entomology and University of California Davis Cancer Center, University of California, One Shields Avenue, Davis, California 95616

Received June 8, 2010

1,3-Disubstituted ureas possessing a piperidyl moiety have been synthesized to investigate their structure–activity relationships as inhibitors of the human and murine soluble epoxide hydrolase (sEH). Oral administration of 13 1-aryl-3-(1-acylpiperidin-4-yl)urea inhibitors in mice revealed substantial improvements in pharmacokinetic parameters over previously reported 1-adamantylurea based inhibitors. For example, 1-(1-(cyclopropanecarbonyl)piperidin-4-yl)-3-(4-(trifluoromethoxy)phenyl)urea (**52**) showed a 7-fold increase in potency, a 65-fold increase in C_{\max} , and a 3300-fold increase in AUC over its adamantane analogue 1-(1-adamantyl)-3-(1-propionylpiperidin-4-yl)urea (**2**). This novel sEH inhibitor showed a 1000-fold increase in potency when compared to morphine by reducing hyperalgesia as measured by mechanical withdrawal threshold using the *in vivo* carrageenan induced inflammatory pain model.

Introduction

The soluble epoxide hydrolase (sEH,^a EC 3.3.2.3) converts epoxides to the corresponding diols by the catalytic addition of a water molecule. The enzyme is implicated in several disease states for its ability to metabolize fatty acid epoxides such as epoxyeicosatrienoic acids (EETs) and leukotoxin, important endogenous signaling lipids, to less active dihydroxyeicosatrienoic acids (DHETs)¹ and toxic, proinflammatory leukotoxin diols,² respectively. sEH inhibitors are of growing interest for therapeutic use because they have been shown to increase the *in vivo* concentration of EETs and other fatty acid epoxides, resulting in anti-inflammatory,³ antihypertensive,⁴ neuroprotective,⁵ and cardioprotective effects.^{6–8} Several reviews have been published concerning the mechanism of action and diverse biological roles of EETs and the sEH inhibitors that stabilize them.^{9–16} Of particular note, Marino¹⁷ recently reviewed the chemistry of sEH inhibitors and Shen¹⁸ summarized the patent literature in the sEH field.

The prototypical inhibitors dicyclohexylurea and 12-(3-adamantane-1-ylureido)dodecanoic acid (AUDA), while potent *in vitro*, suffer from poor physical properties and poor *in vivo* stability. Amides, carbamates, and other pharmacophores^{17,18} have been explored as alternative pharmacophores in an attempt to improve physical properties and show structure–activity relationships similar to those of ureas, but the disubstituted ureas remain the most studied class of inhibitors because of their high potency^{19–23} and promising

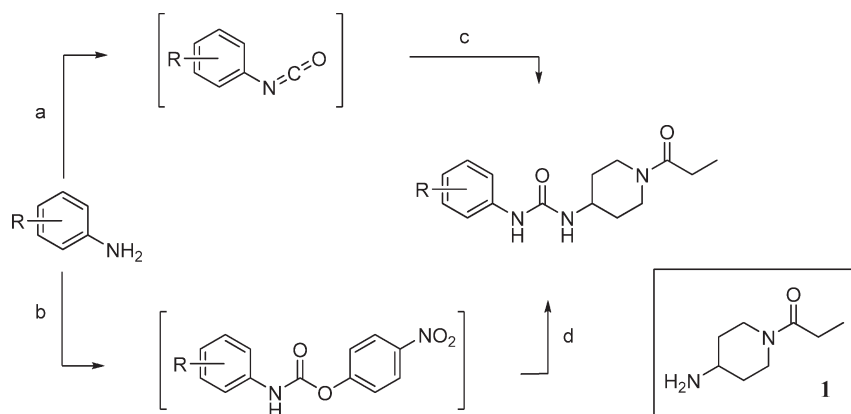
pharmacokinetics.^{24,25} Although earlier studies found that trisubstituted ureas had reduced potency,^{9,26} with proper substituents piperidine based trisubstituted ureas have been found to be potent inhibitors of the enzyme.^{27–30} In the past year several other promising pharmacophores have been reported.^{17,18,21,28,31} We previously reported inhibitors incorporating a polar moiety, such as an *N*-acylpiperidine or cyclohexyloxybenzoic acid, to one side of the urea, which yielded a substantial improvement in water solubility and oral bioavailability while retaining excellent potency.^{24,25,32,33} The adamantyl moiety retained in many of these potent second-generation sEH inhibitors provided sensitive characteristic mass spectral fragmentation. However, this moiety is prone to rapid metabolism, often leading to low drug concentrations in the blood and short *in vivo* half-life.

Replacement of the adamantyl group with a phenyl ring has been explored in our earlier work and has yielded several highly potent inhibitors, warranting further investigation.^{25,33,34} Thus, in this study, we further investigated urea based sEH inhibitors by optimizing the 1-aryl-3-(1-acylpiperidin-4-yl)urea core structure. On the basis of the reported 2-fold increase in potency of the *N*-propionylpiperidine over the *N*-acetyl piperidine in a group of adamantylureas,^{25,32} a series of inhibitors conserving the *N*-propionylpiperidine moiety was synthesized to probe the SAR of the aryl group. Additional inhibitors conserving 4-trifluoromethoxyphenyl as the aryl group and varying in *N*-acylpiperidine or *N*-sulfonylpiperidine substitution were synthesized to examine the effects of polar and basic side chains on potency.

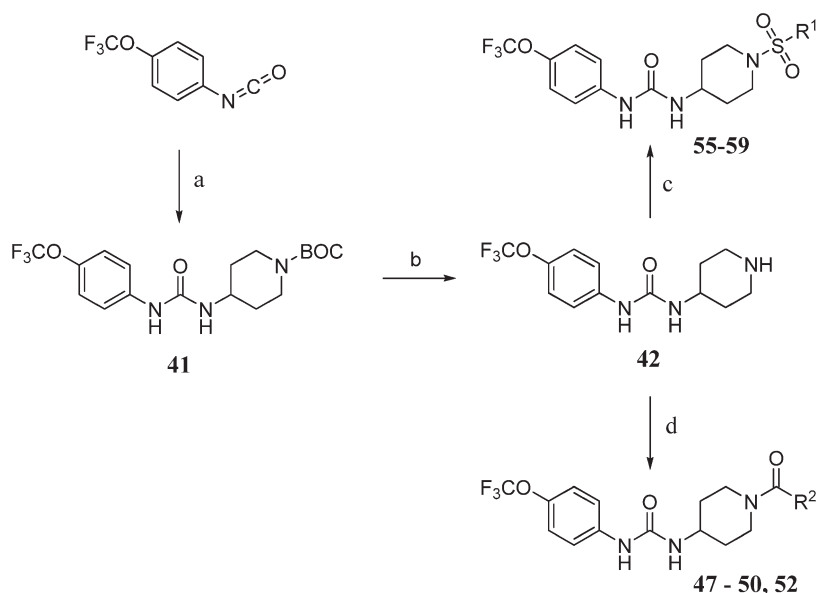
Inhibitors were first screened for potency *in vitro* against homogeneous recombinant murine sEH and human sEH, and their octanol–water partition coefficients were determined to help direct our search for more “druglike” molecules. Pharmacokinetic screening by oral cassette dosing was then undertaken in mice for 13 piperidines exhibiting

*To whom correspondence should be addressed. Phone: 530-752-7519. Fax: 530-752-1537. E-mail: bdhammock@ucdavis.edu.

^a Abbreviations: sEH, soluble epoxide hydrolase; EETs, epoxyeicosatrienoic acids; DHETs, dihydroxyeicosatrienoic acids; AUDA, 12-(3-adamantane-1-ylureido)dodecanoic acid; SAR, structure–activity relationship; $t_{1/2}$, half-life; C_{\max} , maximum concentration; IC_{50} , half maximal inhibitory concentration; AUC, area under the curve; LOQ, limit of quantitation.

Scheme 1. Synthesis of *N*-Propionylpiperidine Analogues^a

^a Reaction conditions: (a) triphosgene, DCM, sat. NaHCO₃ or 1 N NaOH, sat. NaCl, 0 °C, 10 min; (b) 4-nitrophenyl chloroformate, Et₃N, THF, 0–50 °C, 1–3 h; (c) **1**, THF, 0 °C to room temp, 1–24 h; (d) **1**, DMF, 70 °C, 4 h.

Scheme 2. Synthesis of *N*-Acyl and *N*-Sulfonylpiperidine Analogues^a

^a Reagents and conditions: (a) 1-BOC-4-aminopiperidine, THF, 0 °C to room temp, 12 h; (b) 1 N HCl in MeOH, reflux, 3 h; (c) R¹SO₂Cl, Et₃N, THF, 0 °C to room temp, 12 h; (d) EDCI, R²COOH, DMAP, DCM, room temp, 12–24 h.

good *in vitro* potency and desirable structural characteristics. In addition several bridging compounds were studied to relate this study to previous publications. The *in vivo* anti-inflammatory and analgesic bioactivity of one sEHi were evaluated using carrageenan induced inflammatory pain model.

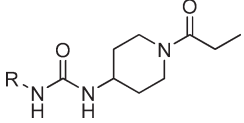
Chemistry

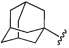
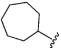
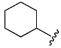

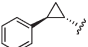
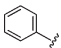
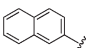
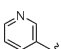
Scheme 1 outlines the two general synthetic routes used to form the unsymmetrical 1,3-disubstituted urea pharmacophore. Aryl isocyanates were purchased or formed from their corresponding anilines by reaction with triphosgene in the presence of aqueous base.³⁵ The heptafluoroisopropylanilines required for compounds **38** and **39** were prepared as described.³⁶

Amine **1** was prepared from 4-aminopiperidine by protection of the primary amine as its benzylimine,³⁷ reaction with propionyl chloride in the presence of triethylamine, and subsequent deprotection. All isocyanates were reacted with amine **1** to give the desired (1-propionylpiperidin-4-yl)ureas **2–16**,

18–21, and **24–40**. Saponification of methyl ester **21** with methanolic NaOH afforded benzoic acid **22**. Phenol **23** was prepared via 4-benzyloxy isocyanate to avoid formation of a carbamate side product.

Compounds **17** and **31** were prepared by conversion of the corresponding aniline to the intermediate 4-nitrophenyl carbamate, which was then reacted with amine **1** to give the desired urea. Intermediate **41** (Scheme 2) was prepared by the reaction of 4-trifluoromethoxyphenyl isocyanate with 1-BOC-4-aminopiperidine. BOC deprotection gave piperidine **42**, which was converted to *N*-acyl compounds **47–50** and **52** by an EDCI mediated coupling reaction with the respective carboxylic acid.³⁷ Acetylpiperazine **51** was prepared by debenzoylation of **50** and subsequent *N*-acetylation. Trifluoroacetyl compound **53** was prepared by the reaction of intermediate **42** with ethyl trifluoroacetate. Trihydroxybenzoyl compound **54** was prepared by coupling of **42** with tris-*O*-benzyl protected gallic acid (**44**) followed by hydrogenolysis.^{38,39} Intermediate **42** was also converted to *N*-sulfonyl compounds **55–59** by reaction with the respective sulfonyl chlorides.

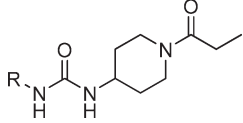
Table 1. Alkyl, Carbocycle, and Unsubstituted Aryl Analogues


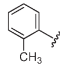
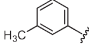
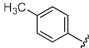
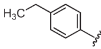
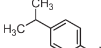
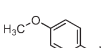
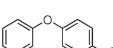
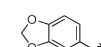
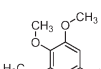
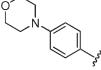
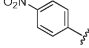
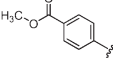
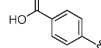
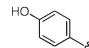
| Compd | R | IC ₅₀ (nM) ^a | | logP (±0.5) ^b |
|-------|---|------------------------------------|--------|-----------------------------|
| | | Human | Murine | |
| 2 |  | 2.8 | 1.2 | 3.1 |
| 3 |  | 3.9 | 0.9 | 2.3 |
| 4 |  | 12 | 3.5 | 1.8 |
| 5 |  | 3.2 | 0.4 | 3.5 |
| 6 |  | 2.7 | 7.4 | 1.8 |
| 7 |  | 130 | 49 | 1.3 |
| 8 |  | 3.0 | 4.2 | 2.4 |
| 9 |  | 3,800 | >5,000 | nd ^c |

^aIC₅₀ values were determined with a fluorescent assay using homogeneous recombinant murine and human enzymes (see methods section). ^bConfidence refers to log *P* value. See Supporting Information for full explanation. ^cThe HPLC method used is limited to log *P* values greater than zero.

Results and Discussion

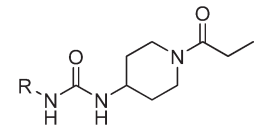
Effects of Phenyl Substitution on Potency. In Tables 1–4 a partial structure is shown at the top and the R groups are detailed. Full structures are shown in the Supporting Information along with detailed synthetic methods. Previous studies have shown that the steric bulk of groups adjacent to the urea is positively correlated with inhibitor potency,²⁶ as was again observed for compounds **2–8** (Table 1). This effect is more directly attributed to the hydrophobicity of these groups, as indicated by the positive correlation between potency (–log IC₅₀) and log *P* values ($r = 0.67/0.87$, human/murine) for simple side chains in **2–8**. Although replacing the cyclohexyl ring (**4**) with a more compact phenyl ring (**7**) caused an 11-fold drop in potency against the human enzyme, substitution of the phenyl ring allowed access to electronically and sterically diverse structures (Tables 2 and 3). Compound **6** provides a bridging structure to recent literature compounds.²⁷ Inclusion of a pyridine on the left side of the molecule as in compound **9** resulted in a dramatic reduction in potency in the piperidine series, although good potency of such pyridines are reported in the patent literature,^{17,18} and other reports.^{22,27–30} Inclusion of such polar groups are attractive to improve physical properties, pharmacokinetic properties, and ease of formulation.

Table 2. Substituted Phenyl Analogues


| Compd | R | IC ₅₀ (nM) | | logP (±0.5) |
|-------|---|-----------------------|--------|----------------|
| | | Human | Murine | |
| 10 |  | 1,700 | >5,000 | 1.6 |
| 11 |  | 40 | 8.7 | 1.8 |
| 12 |  | 43 | 55 | 1.8 |
| 13 |  | 8.3 | 1.3 | 2.3 |
| 14 |  | 2.8 | 3.3 | 2.8 |
| 15 |  | 87 | 8.7 | 1.0 |
| 16 |  | 3.5 | 0.4 | 2.8 |
| 17 |  | 61 | 100 | 1.1 |
| 18 |  | >5,000 | >5,000 | 0.8 |
| 19 |  | 2,000 | 650 | 0.2 |
| 20 |  | 38 | 97 | 1.7 |
| 21 |  | 140 | 64 | 1.6 |
| 22 |  | 330 | 1,000 | 0.4 |
| 23 |  | 406 | 1,400 | 0.0 |

Compared to the unsubstituted phenyl compound **7**, the inhibition potencies increased dramatically when small non-polar meta or para (**11**, **12**) substituents were added. Their presence at the ortho position (**10**) has a clear negative effect on potency. Increasing the size of the hydrophobic para substituent in compounds **12–16** yielded a 3- to 46-fold increase in potency over **7**. However, the presence of polar para

Table 3. Halophenylurea Analogues



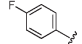
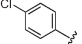
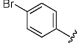
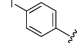
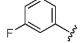
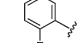
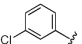
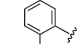
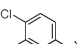
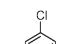
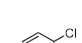
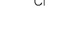



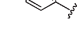
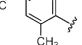
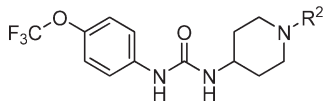
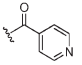
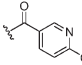
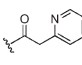
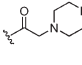
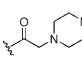
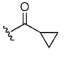
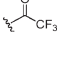
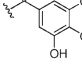
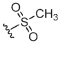
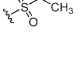
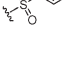
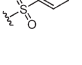
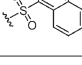
| Compd | R | IC ₅₀ (nM) | | logP (±0.5) |
|-------|---|-----------------------|--------|----------------|
| | | Human | Murine | |
| 24 |  | 79 | 110 | 1.4 |
| 25 |  | 10 | 23 | 2.2 |
| 26 |  | 3.6 | 15 | 2.4 |
| 27 |  | 7.2 | 1.4 | 2.5 |
| 28 |  | 39 | 20 | 1.7 |
| 29 |  | 300 | 780 | 1.6 |
| 30 |  | 21 | 6.6 | 2.2 |
| 31 |  | 1100 | 2900 | 2.0 |
| 32 |  | 3.4 | 0.6 | 2.9 |
| 33 |  | 0.4 | 1.0 | 3.3 |
| 34 |  | >5,000 | >5,000 | 1.3 |
| 35 |  | 4.1 | 2.3 | 3.0 |
| 36 |  | 0.7 | 6.5 | 2.4 |
| 37 |  | 17 | 8.8 | 2.4 |
| 38 |  | 0.4 | 0.7 | 3.5 |
| 39 |  | 17 | 28 | 3.8 |
| 40 |  | 3.7 | 2.8 | 2.5 |

Table 4. N-Acyl and N-Sulfonylpiperidine Analogues



| Compd | R ² | IC ₅₀ (nM) | | logP (±0.5) |
|-------|--|-----------------------|-----------------|----------------|
| | | Human | Murine | |
| 47 |  | 0.7 | 1.3 | 2.4 |
| 48 |  | 0.6 | 0.7 | 2.9 |
| 49 |  | 3.1 | 5.0 | 2.6 |
| 50 |  | 1.5 | 18 | 3.8 |
| 51 |  | 0.5 | 1.2 | 2.4 |
| 52 |  | 0.4 | 0.4 | 2.7 |
| 53 |  | 0.4 | 0.4 | 3.1 |
| 54 |  | 0.5 | 2.7 | 2.0 |
| 55 |  | 2.9 | 2.0 | 2.2 |
| 56 |  | 0.4 | 0.7 | 2.6 |
| 57 |  | 1.8 | 0.4 | 3.1 |
| 58 |  | 0.4 | 0.4 | 3.5 |
| 59 |  | 0.8 | nd ^a | 4.3 |

^a nd = Not determined.

substituents (17–23) resulted in less potent inhibitors. The phenol **23**, a likely metabolite of **15**, was a poor inhibitor presumably because of unfavorable electronic character and polarity. Compound **20** was far less potent than anticipated

because of the high polarity of the nitro functionality, despite having a favorable electron deficient urea. Methyl ester and corresponding carboxylic acid compounds **21** and **22** showed similarly diminished potency. The poor performance of highly polar substituents led us to investigate halophenyl analogues (Table 3). Halogens can increase polarity as a result of their inherent electronegativity and can also serve to block metabolism at particularly reactive sites and reduce metabolism of the aromatic group by decreasing its electron density.

Thus, compounds **24–27** were synthesized to slow metabolic oxidation of the aromatic ring by cytochrome P450 enzymes (CYPs). These compounds also revealed a slight electronic effect on potency, which was less clear in previous studies.^{34,40} The observed increase in potency ($-\log \text{IC}_{50}$) was correlated with electron withdrawing characteristics according to classical Hammett substituent constants ($r = 0.82$) and the ^1H NMR chemical shifts of the urea N–H adjacent to the phenyl ring ($r = 0.77$).⁴¹ This effect, in the absence of confounding steric effects, was well revealed in comparing para versus meta fluorination. *m*-Fluorophenyl (**28**, $\sigma = 0.337$, ^1H NMR δ 8.57) showed a 2-fold and 5-fold lower IC_{50} against the human and murine enzymes, respectively, than *p*-fluorophenyl (**24**, $\sigma = 0.062$, ^1H NMR δ 8.36). Along these lines the 3,5-dichloro substituents yielded a particularly potent sEH inhibitor (**33**, $\sigma = 0.746$, ^1H NMR $\delta = 8.74$). An electron withdrawing group presumably strengthens hydrogen bonding interaction of the urea hydrogen with Asp³³⁴ at the catalytic site of the human enzyme (or Asp³³³ of the murine enzyme) by inductive withdrawal of the nitrogen lone electron pair, further polarizing the urea N–H bond. Fine optimization of 3,4- and 3,5-disubstituted electron withdrawing groups should yield additional potent compounds. The fluorinated *p*-isopropyl derivative **38** showed an increase in activity over the corresponding isopropylphenyl derivative **14**. As observed previously⁴⁰ and for the *o*-tolyl compound **10**, ortho mono- or dihalogenation in compounds **29**, **31**, and **34** drastically decreased potency. However, this effect may be mitigable by the addition of a large hydrophobic para substituent, such as perfluoroisopropyl in compound **39**. It is difficult to discern between hydrophobic and electronic contributions to inhibitor potency in vitro. Experimental $\log P$ values and calculated molar volumes (data not shown) are highly predictive of the relative potencies of the carbocyclic, alkylphenyl, and phenyl ether analogues. However, these criteria do not fully account for the high potency observed for halophenyl compounds, highlighting an electronic contribution to inhibitor potency.

Comparison of Piperidine N-Substituents. The 4-trifluoromethoxyphenyl moiety was used as a metabolically stable replacement for the adamantyl ring of our earlier generation of inhibitors^{25,33,40} and was thus conserved in order to investigate N-substitution of the piperidine moiety. *N*-Acyl and *N*-sulfonyl substitution of the 1-(piperidin-4-yl)-3-(4-(trifluoromethoxy)phenyl)urea core structure (intermediate **42**) yielded multiple highly potent inhibitors (Table 4).

Compounds **47–51** demonstrated the feasibility of introducing a basic nitrogen to allow formulation of the inhibitor as a salt. Analogues **55** and **56** indicate that the sulfonamide group is a good isosteric replacement for the amide, yielding comparably potent inhibitors. These two functional groups may provide valuable pharmacokinetic and pharmacodynamic differences. While bulky substituents on the phenyl moiety improve potency, bulky N-substitution on the piperidine (**50**,

Table 5. Pharmacokinetic Screening Results^a

| compd | C_{\max} (nM) | T_{\max} (min) | $t_{1/2}$ (min) | AUC _t ($\times 10^4$ nM·min) |
|-------------------|-----------------|------------------|-----------------|---|
| AUDA ^b | 14 | 80 | 126 | 0.3 |
| 2 | 138 | 45 | 78 | 1.9 |
| 3 | 2770 | 60 | 50 | 35 |
| 4 | 4600 | 50 | 56 | 58 |
| 12 | 5570 | 30 | 72 | 92 |
| 13 | 4810 | 30 | 56 | 74 |
| 14 | 5860 | 50 | 58 | 95 |
| 15 | 13000 | 70 | 82 | 283 |
| 24 | 8410 | 83 | 378 | 467 |
| 25 | 18300 | 188 | 381 | 1360 |
| 27 | 3790 | 440 | 881 | 375 |
| 35 | 5940 | 230 | 814 | 516 |
| 40 | 17400 | 220 | 980 | 1400 |
| 52 | 8900 | 190 | 1180 | 985 |

^a Values are from single oral cassette dosing at 5 mg/kg in 120–150 μL of 20% PEG400 v/v in oleic ester rich triglyceride. Full pharmacokinetic profiles are shown in Figures S1–S3, and plots of murine AUC as a function of the IC_{50} on the human enzyme and the murine enzyme are shown in Figures S4 and S5 in the Supporting Information. ^b AUDA gave biphasic kinetics.

51, **54**, **57–59**) did not substantially improve potency over such compounds as **40** or **56**. Although bulky N-substitution leads to some increases in potency, previous studies in canines showed that large N-substituents decreased blood levels dramatically following oral administration.²⁵

Small *N*-acyl or *N*-sulfonyl substituents may improve hydrophobic interaction with the enzyme while minimizing the need for conformational change upon entry into the catalytic tunnel. The presence of a small hydrophobic group (**52**, **53**) improved potency approximately 9-fold over compound **40** and reached the LOQ of our in vitro assay. Although highly potent, the hydrolytic instability of the trifluoroacetamide **53** makes it unsuited for in vivo use. Cyclopropanecarboxamide **52**, however, is a reasonable modification that improves metabolic stability over propionamide **40** without significantly increasing the molecular weight or $\log P$ value. Proper substitution on the phenyl ring is crucial for attaining good potency. A varying degree of polarity, bulk, and basicity is extremely well tolerated by the target enzyme if attached to the piperidine nitrogen, away from the urea pharmacophore.

Pharmacokinetic Screening in Mice. Carbocycle and phenyl substituted ureas significantly improved pharmacokinetics in comparison to the earlier inhibitors AUDA,³⁴ AEPD (1-[1-acetylpiperidin-4-yl]-3-adamantanylurea),^{24,32} and 1-(1-adamantyl)-3-(1-propionylpiperidin-4-yl)urea compound **2**³² (Table 5 and Supporting Information). Our results suggest that the adamantane ring is generally less favorable, in terms of ADME, than other groups. The results also demonstrate that molecules can be fine-tuned to optimize ADME and physical properties while retaining high inhibitory potency on the enzyme.

Replacing the adamantane with cycloalkanes in compounds **2–4** resulted in substantially higher blood levels. For example, substitution of the adamantyl ring (**2**) with a cyclohexyl ring (**4**) resulted in a 33-fold and 81-fold increase in C_{\max} and AUC, respectively, while the cycloheptyl ring (**3**) increased exposure while retaining potency on the recombinant enzymes (Figures S4 and S5). Likewise, the 4-alkylphenyl compounds (**12–14**) showed improved PK profiles similar to that of compound **4**. Interestingly, homologation of the para-alkyl group altered potency in vitro, with **14**

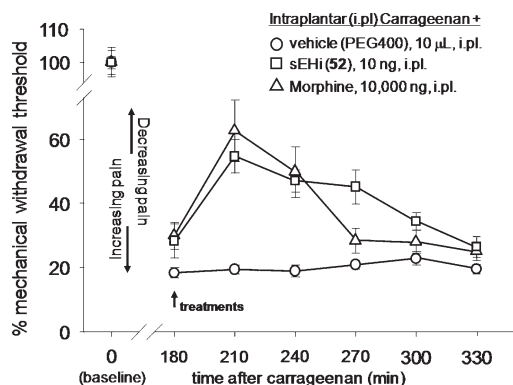


Figure 1. The soluble epoxide hydrolase inhibitor **52** (sEHi) reduces local inflammatory pain at a far lower dose than morphine. The inflammatory agent carrageenan was administered at time 0, resulting in a stable hyperalgesic response for the duration of the experiment. Zero time points represent normal response to pain. Treatment at 180 min after carrageenan with either morphine or compound **52** reversed symptoms. Standard deviation represents the average of six animals with regard to mechanical withdrawal threshold.

exhibiting the lowest IC_{50} against both enzymes, but did not significantly alter PK. The 4-methoxyphenyl (**15**) surprisingly showed a further increase in C_{max} and AUC by approximately 2-fold and 3-fold, respectively, over compounds **3** and **12–14**, suggesting that an ether substituent helps to improve absorption and favorably alters metabolism. Compounds **2–4** and **12–15** were largely cleared in approximately 8 h.

The 4-halophenyl compounds **24**, **25**, and **27** are more persistent than the former materials and have drastically increased C_{max} and AUC, supporting our hypothesis that metabolism of the 1-aryl-3-(1-propionylpiperidin-4-yl)urea core structure occurs predominantly at the phenyl moiety. To bridge these data to the anticancer drug sorafenib,⁴² which is also a potent sEH inhibitor,⁴³ compound **35** was tested.

The sorafenib-like compound **35** exemplifies excellent stability with two electron withdrawing groups on the phenyl ring.⁴³ Interestingly, the chlorophenyl compound **25** showed significantly better PK than the other monohalogenated analogues tested. While the lower C_{max} and AUC of 4-iodophenyl compound **27** is likely a consequence of its poor solubility, the large difference between 4-fluorophenyl (**24**) and 4-chlorophenyl (**25**) suggests that the improved ADME of **25** is a result of favorable polarity and electronics.

Pain Reduction in Mice. Compound **52** was selected for biological studies as showing both high potency and good pharmacokinetics in mice (Figures S1–S5). Several studies have demonstrated a dramatic reduction of inflammation by sEH inhibitors both alone and when combined with aspirin and nonsteroidal anti-inflammatory drugs.³ Thus, compound **52** was tested in an inflammation driven pain model (Figure 1).

For this study local inflammatory pain was induced by a single, intraplantar injection of carrageenan in rats. The animals' mechanical withdrawal thresholds, expressed as a percent of control, were measured before (baseline) and 3 h after carrageenan administration. At this time vehicle or compounds were administered into the plantar surface of the inflamed paw, indicated by an arrow, in a volume of 10 μ L. Mechanical withdrawal thresholds were then monitored ($n = 6$ per group). Intraplantar carrageenan led to significant pain observed as a dramatic decrease in mechanical withdrawal

threshold of animals. This state was sustained over the course of the experiment. The sEHi (10 ng/paw) and morphine (10 000 ng/paw) significantly reversed carrageenan induced pain in a time dependent manner, although the sEHi was more stable than morphine (sEHi vs morphine, ANOVA followed by Dunnett's two-sided t test, $p > 0.3$) 270 min after treatment even though the dose of the sEH inhibitor was 1000 lower than the morphine dose.

Conclusion

The sEH inhibitors are promising pharmacological leads based on their successful use in multiple models of human disease including prevention and reversal of cardiac hypertrophy^{16,44} and a dramatic reduction of inflammation and pain when used either alone or with nonsteroidal anti-inflammatory drugs.^{3,45} As discussed in the Introduction, there are several excellent lead structures under investigation as sEH inhibitors.^{17,18} Disubstituted urea sEH inhibitors with substituted piperidines as the secondary pharmacophore were selected as the focus of this study because they are small, druglike, conformationally restricted structures that are synthetically straightforward.^{25,32} Earlier compounds in this series showed attractive pharmacokinetic properties.^{24,25} Although many criteria are used for the selection of an investigational new drug candidate or a probe for investigating the arachidonic acid cascade in experimental animals, an estimate of exposure indicated by blood levels (Table 5, Figures S1–S3) and enzyme inhibition as an indication of potency (Tables 1–4 and S2) are important considerations as are physical properties. When the potential efficacy of compounds is expressed as a function of exposure in murine blood and potency on the recombinant human enzyme, compound **52** represents an improvement of over 10^4 from the bridging compound AUDA reported 10 years ago (Figure S4).^{9,19} It is important to look at a compound's potency in the model species being used, and a similar trend with a 10^5 improvement is seen when murine potency data are used (Figure S5). Evaluation of potency in the model species used is critical. For example, there is a good correlation between data on the recombinant mouse and rat enzymes, while there is not a perfect correlation between IC_{50} on human and murine enzymes ($r^2 = 0.77$; $\rho = 0.80$; Figure S6), and a poor correlation among canine, rodent, and human enzymes particularly for the piperidine containing sEH inhibitors.²⁵

Figure S3 compares the blood pharmacokinetic profile of compound **52** with that of the closely related bridging compound APAU previously published from this laboratory.³² The activity of these acylpiperidine compounds is similar on the human and murine recombinant enzymes, but compound **52** is about 30 times more potent on the human than the murine enzyme.^{25,32} The data in Figure S3 indicate a very short half-life and small AUC for APAU. When the AUC/ IC_{50} is used as a metric, there is a 5500-fold improvement with compound **52** over the earlier APAU.

Thus, multiple compounds in this series and particularly compounds such as **40** and **52** should be reasonable compounds to use in murine models of disease. Both inhibitors have similar potencies on the rodent and human enzyme and reasonable pharmacokinetics. In particular the data in Figure 1 demonstrate the efficacy of compound **52** in a pain model. More broadly, these data demonstrate rational ways to fine-tune inhibitors in this series as potential therapeutics. It is possible that combinations of these and related structural

units will yield highly potent inhibitors and with pharmacokinetics fine-tuned for use in various species.

Experimental Section

General. All reagents and solvents were purchased from commercial suppliers and were used without further purification. All reactions were performed under an inert atmosphere of dry nitrogen. Flash chromatography was performed on silica gel using a dry loading technique, where necessary for poorly soluble products, and elution with the appropriate solvent system. Melting points were determined using an OptiMelt melting point apparatus and are uncorrected. ^1H NMR spectra were collected using a Bruker Avance 500 MHz spectrometer or Varian Mercury 300 MHz spectrometer. Accurate masses were measured using a Micromass LCT ESI-TOF-MS equipped with a Waters 2795 HPLC. The log *P* and purity analyses were performed using a Hewlett-Packard 1100 HPLC instrument equipped with a diode array detector. A Phenomenex Luna 150 mm \times 4.6 mm, 5 μm , C-18 column was used for all HPLC analyses. For purity analysis, final products were dissolved in MeOH/H₂O (3:1, v/v) at 10 $\mu\text{g}/\text{mL}$, and 100 μL injections were analyzed in triplicate by HPLC–UV with detection at 210, 230, 254, and 290 nm. HPLC conditions were the same as those for log *P* determination (see below). Purity was judged as the percent of total peak area for each wavelength. The lowest observed purity is reported. Compounds were also judged to be pure based on thin layer chromatography visualized with short wave UV and stained with basic potassium permanganate. Compounds were $\geq 95\%$ pure by HPLC–UV except where specifically noted (see Supporting Information). All compounds were evaluated by LC–MS and NMR specifically to ensure that there was no symmetrical urea impurity present, since these compounds can be very active.

log *P* Determination. Octanol–water partition coefficients were determined by an HPLC method following OECD Guideline 117. The accepted error for this method is ± 0.5 log unit of shake flask values (OECD Guideline 107). Isocratic MeOH/H₂O (3:1, v/v), 50 mM ammonium acetate in MeOH/H₂O (3:1, v/v) adjusted to pH 9.0, and MeOH/H₂O (3:1, v/v) adjusted to pH 3.0 with H₃PO₄ were used for neutral, basic, and acidic analytes, respectively, with a flow rate of 0.75 mL/min. The HPLC method was validated using compounds **24** and **54**, which were found to have log *P* values of 1.9 and 2.3, respectively, using the shake flask method (OECD Guideline 107).²⁵ Many algorithms for calculation of log *P* values experience difficulty with urea compounds. For example the r^2 for the correlation for the ClogP values and shake flask values (OECD Guidelines 107 and 122) was < 0.3 ,²⁵ while the correlation with the HPLC method used herein was ~ 0.7 (Figure S7).

Method A: Synthesis of Aryl and Alkyl Isocyanates. The aniline or amine (1 mmol) was added to an ice cold, stirred biphasic mixture of DCM (10 mL) and saturated sodium bicarbonate (10 mL) or 1 N NaOH (3 mL) in brine (7 mL) where noted. Stirring was stopped momentarily, triphosgene (0.37 equiv) in DCM (1 mL) added via syringe to the lower DCM layer, and stirring continued for 10 min. The DCM layer was removed and filtered through a bed of magnesium sulfate. The filtrate was evaporated to afford the corresponding isocyanate, which was used without further purification.

Method B: Synthesis of Ureas via Isocyanate. The isocyanate (1 mmol) was dissolved or suspended in dry THF (3–5 mL) and cooled in an ice bath. The amine (1 mmol) was dissolved in dry THF (1 mL) and slowly added to the reaction. Stirring was continued for 1–24 h at room temperature. The reaction was quenched with dilute HCl (or water where the BOC group was present) and extracted into ethyl acetate. The combined organic phase was dried, evaporated, and purified.

Method C: Synthesis of Ureas via 4-Nitrophenylcarbamate. To an ice cold solution of 4-nitrophenyl chloroformate (1 equiv) in

dry THF was added Et₃N (1.3 equiv), and the appropriate aniline (1 equiv) was dissolved in dry THF. The mixture was allowed to warm to room temperature, stirred for 30 min, and then filtered. The filtrate was evaporated and dissolved in DMF. Amine **1** was added and the mixture warmed to 50 °C for 1–3 h. The mixture was cooled to room temperature, diluted with ethyl acetate, and the organic phase washed with 1 N NaOH until the wash was free of yellow *p*-nitrophenol. The organic phase was dried, evaporated, and purified.

Method D: Synthesis of *N*-Acylpiperidine Analogues. To a solution of **41** (1 equiv) in DCM were added the corresponding carboxylic acid (1.1 equiv), DMAP (1 equiv), and EDCI (1.1 equiv). The mixture was stirred for 12–24 h at room temperature. Neutral products were worked up by partition with EtOAc and 1 N HCl (basic products by partition with saturated sodium bicarbonate and EtOAc), and the organic phase was dried, evaporated, and purified.

Method E: Synthesis of *N*-Sulfonylpiperidine Analogues. To a solution of **41** (152 mg, 0.5 mmol) in dry THF (5 mL) were added Et₃N (1.3 equiv) and the corresponding sulfonyl chloride (1 equiv) in dry THF (1 mL). The mixture was stirred for 12 h, quenched with 1 N HCl, and filtered to collect the resulting precipitate, which was further purified.

Enzyme Purification. Recombinant murine and human sEH were produced in a polyhedron positive baculovirus expression system, and they were purified by affinity chromatography as previously reported.^{46–48}

IC₅₀ Assay Conditions. IC₅₀ values were determined using a sensitive fluorescent based assay.⁴⁹ Cyano(2-methoxynaphthalen-6-yl)methyl *trans*-(3-phenyloxyran-2-yl)methylcarbonate (CMNPC) was used as the fluorescent substrate. Human sEH (1 nM) or murine sEH (1 nM) was incubated with the inhibitor for 5 min in pH 7.0 Bis-Tris/HCl buffer (25 mM) containing 0.1 mg/mL BSA at 30 °C prior to substrate introduction ([S] = 5 μM). Activity was determined by monitoring the appearance of 6-methoxy-2-naphthaldehyde over 10 min by fluorescence detection with an excitation wavelength of 330 nm and an emission wavelength of 465 nm. Reported IC₅₀ values are the average of three replicates with at least two data points above and at least two below the IC₅₀. The fluorescent assay as performed here has a standard error between 10% and 20%, suggesting that differences of 2-fold or greater are significant.⁴⁹

Pharmacokinetic (PK) Studies. Male CFW mice (7 week old, 24–30 g) were purchased from Charles River Laboratories. All the experiments were performed according to protocols approved by the Animal Use and Care Committee of University of California, Davis. Inhibitors (1 mg each) were dissolved in 1 mL of oleic ester-rich triglyceride containing 20% polyethylene glycol (average molecular weight: 400) to give a clear solution for oral administration. Since many of these compounds are high melting and relatively water insoluble, it is important that they are in true solution to study their pharmacokinetics. The 20% PEG 400 in oleic ester rich triglyceride gave true solutions for all compounds reported. To avoid ill defined levels of linoleate esters (18:2) in the vehicle, we used the synthetic triglyceride of oleic esters (18:1) or triolein for vehicle. Cassette 1 contained compounds **2**, **24**, **25**, and **27**, cassette 2 compounds **12**, **13**, and **14**, cassette 3 compounds **3**, **4**, and AUDA, cassette 4 compounds **2**, **15**, and **35**, and cassette 5 compounds **40** and **52**. Each cassette was orally administered to three or four mice at a dose of 5 mg/kg in 120–150 μL of vehicle depending on animal weight. Blood (10 μL) was collected from the tail vein using a pipet tip rinsed with 7.5% EDTA (K3) at 0, 0.5, 1, 1.5, 2, 4, 6, 8, 24 h after oral dosing with the inhibitor. The blood samples were prepared according to the methods detailed in our previous study.²⁴ Blood samples were analyzed using an Agilent 1200 series HPLC instrument equipped with a 4.6 mm \times 150 mm Inertsil ODS-4 3 μm column (GL Science Inc., Japan) held at 40 °C and coupled with an Applied Biosystems 4000 QTRAP hybrid, triple-quadrupole mass spectrometer. The instrument was equipped with a linear

ion trap and a Turbo V ion source and was operated in positive ion MRM mode (see Table S1). The solvent system consisted of water/acetic acid (999/1 v/v, solvent A) and acetonitrile/acetic acid (999/1 v/v, solvent B). The gradient was begun at 30% solvent B and was linearly increased to 100% solvent B in 5 min. This was maintained for 3 min, then returned to 30% solvent B in 2 min. The flow rate was 0.4 mL/min. The injection volume was 10 μ L, and the samples were kept at 4 °C in the autosampler. Optimized conditions for mass spectrometry are in Table S1.

For clarity standard deviation is not included in Figure S1. There is less than 5% variation in compound levels in replicate blood samples from the same mice. Thus, the standard deviation shown in Figure S2A–F represents variation among mice treated with the same compound. The PK parameters of individual mice were calculated by fitting the time dependent curve of blood inhibitor concentration (Figure S2) to a noncompartmental analysis with the WinNonlin software (Pharsight, Mountain View, CA). Parameters determined include the time of maximum concentration (T_{max}), maximum concentration (C_{max}), half-life ($t_{1/2}$), and area under the concentration–time curve to terminal time (AUC_t). In separate studies to determine dose linearity of selected compounds, pharmacokinetic parameters determined by cassette dosing were found to be predictive of results from dosing individual compounds.^{24,50} Figure S3 compares the pharmacokinetics of compound **52** with that of the bridging compound APAU.^{24,25,32} Graphs of exposure as a function of potency are shown in Figures S4 and S5.

Inflammatory Pain Model. This study was approved by UC Davis Animal Care and Use Committee. Male Sprague–Dawley rats weighing 250–300 g were obtained from Charles River Inc. and maintained in UC Davis animal housing facilities with ad libitum water and food on a 12 h/12 h light–dark cycle. Behavioral nociceptive testing was conducted by assessing mechanical withdrawal threshold using an electronic von Frey anesthesiometer apparatus (IITC, Woodland Hills, CA).⁴⁵ The controller was set to “maximum holding” mode so that the highest applied force (in gram) upon withdrawal of the paw was displayed. Three measurements were taken at 1–2 min interstimulus intervals. Data were normalized to percentage values using the formula (mechanical withdrawal threshold (g) \times 100)/(mechanical withdrawal threshold (g)) before carrageenan. Compound **52** was tested using the intraplantar carrageenan elicited inflammatory pain model. Following baseline measurements, carrageenan (50 μ L, 1% solution of carrageenan) was administered into the plantar area of one hind paw. Three hours following this, postcarrageenan responses were determined. Immediately after, the vehicle (10 μ L of PEG400), the sEH inhibitor, or morphine sulfate (10 μ g in 10 μ L saline) was administered into the same paw by intraplantar injection in a volume of 10 μ L. Responses following compound administration were monitored over the course of 2.5 h.

Acknowledgment. We thank Dr. Jozsef Lango for assistance with accurate mass determination. This work was supported in part by NIEHS Grant R01 ES002710, NIEHS/Superfund Basic Research Program Grant P42 ES004699, and NIH/NHLBI Grant R01 HL059699. B.D.H. is a George and Judy Senior Fellow of the American Asthma Foundation.

Supporting Information Available: Blood PK profiles, mass spectrometer parameters, figures of exposure/potency ratios for selected compounds, correlation between IC₅₀ values for human and murine sEH, correlation between experimental and ClogP values, conditions and fragmentation patterns for mass spectrometric analysis, cumulative table of structures, results, and properties for all inhibitors presented, and synthetic details and analytical data. This material is available free of charge via the Internet at <http://pubs.acs.org>.

References

- (1) Spector, A. A.; Fang, X.; Snyder, G. D.; Weintraub, N. L. Epoxyeicosatrienoic acids (EETs): metabolism and biochemical function. *Prog. Lipid Res.* **2004**, *43*, 55–90.
- (2) Moghaddam, M. F.; Grant, D. F.; Cheek, J. M.; Greene, J. F.; Williamson, K. C.; Hammock, B. D. Bioactivation of leukotoxins to their toxic diols by epoxide hydrolase. *Nat. Med.* **1997**, *3*, 562–566.
- (3) Schmelzer, K. R.; Kubala, L.; Newman, J. W.; Kim, I. H.; Eiserich, J. P.; Hammock, B. D. Soluble epoxide hydrolase is a therapeutic target for acute inflammation. *Proc. Natl. Acad. Sci. U.S.A.* **2005**, *102*, 9772–9777.
- (4) Yu, Z. G.; Xu, F. Y.; Huse, L. M.; Morisseau, C.; Draper, A. J.; Newman, J. W.; Parker, C.; Graham, L.; Engler, M. M.; Hammock, B. D.; Zeldin, D. C.; Kroetz, D. L. Soluble epoxide hydrolase regulates hydrolysis of vasoactive epoxyeicosatrienoic acids. *Circ. Res.* **2000**, *87*, 992–998.
- (5) Iliff, J. J.; Alkayed, N. J. Soluble epoxide hydrolase inhibition: targeting multiple mechanisms of ischemic brain injury with a single agent. *Future Neurol.* **2009**, *4*, 179–199.
- (6) Yousif, M. H.; Benter, I. F.; Roman, R. J. Cytochrome P450 metabolites of arachidonic acid play a role in the enhanced cardiac dysfunction in diabetic rats following ischaemic reperfusion injury. *Auton. Autacoid. Pharmacol.* **2009**, *29*, 33–41.
- (7) Katragadda, D.; Batchu, S. N.; Cho, W. J.; Chaudhary, K. R.; Falck, J. R.; Seubert, J. M. Epoxyeicosatrienoic acids limit damage to mitochondrial function following stress in cardiac cells. *J. Mol. Cell. Cardiol.* **2009**, *46*, 867–875.
- (8) Xu, D.; Li, N.; He, Y.; Timofeyev, V.; Lu, L.; Tsai, H. J.; Kim, I. H.; Tuteja, D.; Mateo, R. K. P.; Singapur, A.; Davis, B. B.; Low, R.; Hammock, B. D.; Chiamvimonvat, N. Prevention and reversal of cardiac hypertrophy by soluble epoxide hydrolase inhibitors. *Proc. Natl. Acad. Sci. U.S.A.* **2006**, *103*, 18733–18738.
- (9) Morisseau, C.; Hammock, B. D. Epoxide hydrolases: mechanisms, inhibitor designs, and biological roles. *Annu. Rev. Pharmacol. Toxicol.* **2005**, *45*, 311–333.
- (10) Imig, J. D. Epoxide hydrolase and epoxygenase metabolites as therapeutic targets for renal diseases. *Am. J. Physiol.: Renal Physiol.* **2005**, *289*, 496–503.
- (11) Chiamvimonvat, N.; Ho, C. M.; Tsai, H. J.; Hammock, B. D. The soluble epoxide hydrolase as a pharmaceutical target for hypertension. *J. Cardiovasc. Pharmacol.* **2007**, *50*, 225–237.
- (12) Imig, J. D.; Hammock, B. D. Soluble epoxide hydrolase as a therapeutic target for cardiovascular diseases. *Nat. Rev. Drug Discovery* **2009**, *8*, 794–805.
- (13) Wang, Y.-X. J.; Ulu, A.; Zhang, L.-N.; Hammock, B. D. Soluble epoxide hydrolase in atherosclerosis. *Curr. Atheroscler. Rep.* **2010**, *12*, 174–183.
- (14) Gross, G. J.; Nithipatikom, K. Soluble epoxide hydrolase: a new target for cardioprotection. *Curr. Opin. Invest. Drugs* **2009**, *10*, 253–258.
- (15) Fang, X. Soluble epoxide hydrolase: a novel target for the treatment of hypertension. *Recent Pat. Cardiovasc. Drug. Discovery* **2006**, *1*, 67–72.
- (16) Harris, T. R.; Li, N.; Chiamvimonvat, N.; Hammock, B. D. The potential of soluble epoxide hydrolase inhibition in the treatment of cardiac hypertrophy. *Congestive Heart Failure* **2008**, *14*, 209–224.
- (17) Marino, J. P., Jr. Soluble epoxide hydrolase, a target with multiple opportunities for cardiovascular drug discovery. *Curr. Top. Med. Chem.* **2009**, *9*, 452–463.
- (18) Shen, H. C. Soluble epoxide hydrolase inhibitors: a patent review. *Expert Opin Ther. Pat.* **2010**, *20*, 941–956.
- (19) Morisseau, C.; Goodrow, M. H.; Dowdy, D.; Zheng, J.; Greene, J. F.; Sanborn, J. R.; Hammock, B. D. Potent urea and carbamate inhibitors of soluble epoxide hydrolases. *Proc. Natl. Acad. Sci. U.S.A.* **1999**, *96*, 8849–8854.
- (20) Kim, I. H.; Heirtzler, F. R.; Morisseau, C.; Nishi, K.; Tsai, H. J.; Hammock, B. D. Optimization of amide-based inhibitors of soluble epoxide hydrolase with improved water solubility. *J. Med. Chem.* **2005**, *48*, 3621–3629.
- (21) Xie, Y. L.; Liu, Y. D.; Gong, G. L.; Smith, D. H.; Yan, F.; Rinderspacher, A.; Feng, Y.; Zhu, Z. X.; Li, X. P.; Deng, S. X.; Branden, L.; Vidovic, D.; Chung, C.; Schurer, S.; Morisseau, C.; Hammock, B. D.; Landry, D. W. Discovery of potent non-urea inhibitors of soluble epoxide hydrolase. *Bioorg. Med. Chem. Lett.* **2009**, *19*, 2354–2359.
- (22) Eldrup, A. B.; Soleymanzadeh, F.; Taylor, S. J.; Muegge, I.; Farrow, N. A.; Joseph, D.; McKellop, K.; Man, C. C.; Kukulka, A.; De Lombaert, S. Structure-based optimization of arylamides as inhibitors of soluble epoxide hydrolase. *J. Med. Chem.* **2009**, *52*, 5880–5895.

- (23) Anandan, S. K.; Webb, H. K.; Do, Z. N.; Gless, R. D. Unsymmetrical non-adamantyl *N,N'*-diaryl urea and amide inhibitors of soluble epoxide hydrolase. *Bioorg. Med. Chem. Lett.* **2009**, *19*, 4259–4263.
- (24) Liu, J. Y.; Tsai, H. J.; Hwang, S. H.; Jones, P. D.; Morisseau, C.; Hammock, B. D. Pharmacokinetic optimization of four soluble epoxide hydrolase inhibitors for use in a murine model of inflammation. *Br. J. Pharmacol.* **2009**, *156*, 284–296.
- (25) Tsai, H. J.; Hwang, S. H.; Morisseau, C.; Yang, J.; Jones, P. D.; Kim, I. H.; Hammock, B. D. Pharmacokinetic screening of soluble epoxide hydrolase inhibitors in dogs. *Eur. J. Pharm. Sci.* **2010**, *40*, 222–238.
- (26) McElroy, N. R.; Jurs, P. C.; Morisseau, C.; Hammock, B. D. QSAR and classification of murine and human soluble epoxide hydrolase inhibition by urea-like compounds. *J. Med. Chem.* **2003**, *46*, 1066–1080.
- (27) Shen, H. C.; Ding, F. X.; Deng, Q.; Xu, S.; Chen, H. S.; Tong, X.; Tong, V.; Zhang, X.; Chen, Y.; Zhou, G.; Pai, L. Y.; Alonso-Galicia, M.; Zhang, B.; Roy, S.; Tata, J. R.; Berger, J. P.; Colletti, S. L. Discovery of 3,3-disubstituted piperidine-derived trisubstituted ureas as highly potent soluble epoxide hydrolase inhibitors. *Bioorg. Med. Chem. Lett.* **2009**, *19*, 5314–5320.
- (28) Shen, H. C.; Ding, F. X.; Wang, S.; Deng, Q.; Zhang, X.; Chen, Y.; Zhou, G.; Xu, S.; Chen, H. S.; Tong, X.; Tong, V.; Mitra, K.; Kumar, S.; Tsai, C.; Stevenson, A. S.; Pai, L. Y.; Alonso-Galicia, M.; Chen, X.; Soisson, S. M.; Roy, S.; Zhang, B.; Tata, J. R.; Berger, J. P.; Colletti, S. L. Discovery of a highly potent, selective, and bioavailable soluble epoxide hydrolase inhibitor with excellent *ex vivo* target engagement. *J. Med. Chem.* **2009**, *52*, 5009–5012.
- (29) Kowalski, J. A.; Swinamer, A. D.; Muegge, I.; Eldrup, A. B.; Kukulka, A.; Cywin, C. L.; De Lombaert, S. Rapid synthesis of an array of trisubstituted urea-based soluble epoxide hydrolase inhibitors facilitated by a novel solid-phase method. *Bioorg. Med. Chem. Lett.* **2010**, *20*, 3703–3707.
- (30) Eldrup, A. B.; Soleymanzadeh, F.; Farrow, N. A.; Kukulka, A.; De Lombaert, S. Optimization of piperidyl-ureas as inhibitors of soluble epoxide hydrolase. *Bioorg. Med. Chem. Lett.* **2010**, *20*, 571–575.
- (31) Anandan, S. K.; Do, Z. N.; Webb, H. K.; Patel, D. V.; Gless, R. D. Non-urea functionality as the primary pharmacophore in soluble epoxide hydrolase inhibitors. *Bioorg. Med. Chem. Lett.* **2009**, *19*, 1066–1070.
- (32) Jones, P. D.; Tsai, H. J.; Do, Z. N.; Morisseau, C.; Hammock, B. D. Synthesis and SAR of conformationally restricted inhibitors of soluble epoxide hydrolase. *Bioorg. Med. Chem. Lett.* **2006**, *16*, 5212–5216.
- (33) Hwang, S. H.; Tsai, H. J.; Liu, J. Y.; Morisseau, C.; Hammock, B. D. Orally bioavailable potent soluble epoxide hydrolase inhibitors. *J. Med. Chem.* **2007**, *50*, 3825–3840.
- (34) Morisseau, C.; Goodrow, M. H.; Newman, J. W.; Wheelock, C. E.; Dowdy, D. L.; Hammock, B. D. Structural refinement of inhibitors of urea-based soluble epoxide hydrolases. *Biochem. Pharmacol.* **2002**, *63*, 1599–1608.
- (35) Nowick, J. S.; Holmes, D. L.; Noronha, G.; Smith, E. M.; Nguyen, T. M.; Huang, S. L. Synthesis of peptide isocyanates and isothiocyanates. *J. Org. Chem.* **1996**, *61*, 3929–3934.
- (36) Onishi, M.; Yoshiura, A.; Kohno, E.; Tsubata, K. A Process for Producing Perfluoroalkylaniline Derivatives. EP 1006102, June 7, 2000.
- (37) Sonda, S.; Kawahara, T.; Murozono, T.; Sato, N.; Asano, K.; Haga, K. Design and synthesis of orally active benzamide derivatives as potent serotonin 4 receptor agonist. *Bioorg. Med. Chem.* **2003**, *11*, 4225–4234.
- (38) Dhaon, M. K.; Olsen, R. K.; Ramasamy, K. Esterification of N-protected alpha-amino-acids with alcohol/carbodiimide/4-(dimethylamino)-pyridine. Racemization of aspartic and glutamic acid derivatives. *J. Org. Chem.* **1982**, *47*, 1962–1965.
- (39) Ren, Y.; Himmeldirk, K.; Chen, X. Synthesis and structure–activity relationship study of antidiabetic penta-*O*-galloyl-D-glucopyranose and its analogues. *J. Med. Chem.* **2006**, *49*, 2829–2837.
- (40) Hwang, S. H.; Morisseau, C.; Do, Z.; Hammock, B. D. Solid-phase combinatorial approach for the optimization of soluble epoxide hydrolase inhibitors. *Bioorg. Med. Chem. Lett.* **2006**, *16*, 5773–5777.
- (41) Correlations were determined from plots of $-\log IC_{50}$ vs Hammett constants and 1H NMR chemical shifts. Compounds **7**, **12**, **15**, **24–28**, **30**, **32**, and **33** were examined to minimize possible confounding effects on inhibitor potency, such as steric bulk, high polarity, and ortho substitution.
- (42) Zhong, H. Z.; Bowen, J. P. Molecular design and clinical development of VEGFR kinase inhibitors. *Curr. Top. Med. Chem.* **2007**, *7*, 1379–1393.
- (43) Liu, J.-Y.; Park, S.-H.; Morisseau, C.; Hwang, S. H.; Hammock, B. D.; Weiss, R. H. Sorafenib has soluble epoxide hydrolase inhibitory activity, which contributes to its effect profile in vivo. *Mol. Cancer Ther.* **2009**, *8*, 2193–2203.
- (44) Ai, D.; Pang, W.; Li, N.; Xu, M.; Jones, P. D.; Yang, J.; Zhang, Y.; Chiamvimonvat, N.; Shyy, J. Y.-J.; Hammock, B. D.; Zhu, Y. Soluble epoxide hydrolase plays an essential role in angiotensin II-induced cardiac hypertrophy. *Proc. Natl. Acad. Sci. U.S.A.* **2009**, *106*, 564–569.
- (45) Inceoglu, B.; Jinks, S. L.; Ulu, A.; Hegedus, C. M.; Georgi, K.; Schmelzer, K. R.; Wagner, K.; Jones, P. D.; Morisseau, C.; Hammock, B. D. Soluble epoxide hydrolase and epoxyeicosatrienoic acids modulate two distinct analgesic pathways. *Proc. Natl. Acad. Sci. U.S.A.* **2008**, *105*, 18901–18906.
- (46) Beetham, J. K.; Tian, T. G.; Hammock, B. D. cDNA cloning and expression of a soluble epoxide hydrolase from human liver. *Arch. Biochem. Biophys.* **1993**, *305*, 197–201.
- (47) Grant, D. F.; Storms, D. H.; Hammock, B. D. Molecular-cloning and expression of murine liver soluble epoxide hydrolase. *J. Biol. Chem.* **1993**, *268*, 17628–17633.
- (48) Wixtrom, R. N.; Silva, M. H.; Hammock, B. D. Affinity purification of cytosolic epoxide hydrolase using derivatized epoxy-activated sepharose gels. *Anal. Biochem.* **1988**, *169*, 71–80.
- (49) Jones, P. D.; Wolf, N. M.; Morisseau, C.; Whetstone, P.; Hock, B.; Hammock, B. D. Fluorescent substrates for soluble epoxide hydrolase and application to inhibition studies. *Anal. Biochem.* **2005**, *343*, 66–75.
- (50) Watanabe, T.; Schulz, D.; Morisseau, C.; Hammock, B. D. High-throughput pharmacokinetic method: cassette dosing in mice associated with minuscule serial bleedings and LC/MS/MS analysis. *Anal. Chim. Acta* **2006**, *559*, 37–44.